The Plant Cell, Vol. 29: 1357–1372, June 2017, www.plantcell.org © 2017 ASPB.

Type-B ARABIDOPSIS RESPONSE REGULATORs Specify the Shoot Stem Cell Niche by Dual Regulation of *WUSCHEL* OPEN

Wen Jing Meng,[1] Zhi Juan Cheng,[1] Ya Lin Sang,[1] Miao Miao Zhang, Xiao Fei Rong, Zhi Wei Wang, Ying Ying Tang, and Xian Sheng Zhang[2]

State Key Laboratory of Crop Biology, College of Life Sciences, College of Forestry, Shandong Agricultural University, Taian, Shandong 271018, China

ORCID IDs: 0000-0003-3103-8629 (W.J.M.); 0000-0002-3129-5206 (X.S.Z.)

Plants are known for their capacity to regenerate the whole body through de novo formation of apical meristems from a mass of proliferating cells named callus. Exogenous cytokinin and auxin determine cell fate for the establishment of the stem cell niche, which is the vital step of shoot regeneration, but the underlying mechanisms remain unclear. Here, we show that type-B ARABIDOPSIS RESPONSE REGULATORs (ARRs), critical components of cytokinin signaling, activate the transcription of *WUSCHEL* (*WUS*), which encodes a key regulator for maintaining stem cells. In parallel, type-B ARRs inhibit auxin accumulation by repressing the expression of *YUCCA*s, which encode a key enzyme for auxin biosynthesis, indirectly promoting *WUS* induction. Both pathways are essential for de novo regeneration of the shoot stem cell niche. In addition, the dual regulation of type-B ARRs on *WUS* transcription is required for the maintenance of the shoot apical meristem in planta. Thus, our results reveal a long-standing missing link between cytokinin signaling and WUS regulator, and the findings provide critical information for understanding cell fate specification.

INTRODUCTION

Unlike their animal counterparts, the postembryonic development of higher plants depends on the activity of apical meristems residing at each end of the body (Fletcher and Meyerowitz, 2000; Sena et al., 2009; Moreno-Risueno et al., 2015). In the shoot apical meristem (SAM), pluripotent stem cells reside in a specialized microenvironment termed the stem cell niche, which gives rise to the aerial part of the plant (Aichinger et al., 2012; Zhou et al., 2015). The activity of the shoot stem cell niche is tightly controlled by a feedback loop between the homeodomain transcription factor WUSCHEL (WUS) and the small secreted peptide CLAVATA3 (CLV3) in *Arabidopsis thaliana* (Brand et al., 2000; Schoof et al., 2000). The expression of *CLV3* specifically marks the position of stem cells in the central zone (CZ) (Laux, 2003). *WUS* expression precedes that of *CLV3* during embryogenesis and defines the organizing center (OC) beneath the CZ (Aichinger et al., 2012; Gaillochet et al., 2015). Once produced in the OC cells, WUS proteins move to the CZ to activate *CLV3* expression and stem cell specification (Yadav et al., 2011; Daum et al., 2014). Mutation in *WUS* leads to differentiation of stem cells and loss of the shoot meristem, indicating that this gene is necessary for establishing and maintaining the stem cell niche (Mayer et al., 1998; Aichinger et al., 2012).

Besides the primary shoot meristem, plants are capable of regenerating shoot meristems during their postembryonic development, such as axillary and adventitious shoot meristems (Kerstetter and Hake, 1997; Domagalska and Leyser, 2011; Wang et al., 2014). Six decades ago, Skoog and Miller found that under the induction of exogenous cytokinin and auxin, adventitious shoots could be induced in vitro from a mass of proliferating cells named callus (Skoog and Miller, 1957; Sugimoto et al., 2010; Iwase et al., 2011). This process is defined as de novo shoot regeneration and provides an ideal system for studying the specification of stem cell niche in plants (Duclercq et al., 2011; Iwase et al., 2017). During shoot regeneration, *WUS* expression promotes cell fate transition from callus cells to OC, which is essential for the specification of the shoot stem cell niche and the subsequent establishment of the shoot meristem (Duclercq et al., 2011; Aichinger et al., 2012; Ikeuchi et al., 2016).

Previous studies have revealed that cytokinin and auxin play critical roles in shoot regeneration (Ikeuchi et al., 2016). Incubation on medium containing a high cytokinin-to-auxin ratio activates the expression of *WUS* in callus and lateral root primordia and induces the formation of the shoot meristem (Gordon et al., 2007; Chatfield et al., 2013). The expression of Arabidopsis *His kinases4*, which encodes a cytokinin receptor, precedes and subsequently overlaps with that of *WUS* (Gordon et al., 2009). Mutations in type-B *ARABIDOPSIS RESPONSE REGULATORs* (*ARRs*), key regulators of primary cytokinin response genes, result in reduced shoot regeneration (Ishida et al., 2008; Hwang et al., 2012; Hill et al., 2013; Zhang et al., 2015). By contrast, overexpressing type-A *ARRs* encoding negative regulators of cytokinin signaling suppress shoot formation (Buechel et al., 2010). Moreover, spatial biosynthesis, polar transport, and signaling transduction of auxin are required for shoot regeneration (Gordon et al., 2007; Kareem et al., 2015). Our previous results demonstrated a pattern of auxin and cytokinin essential for shoot meristem induction (Cheng et al., 2013). Cytokinin response signals were progressively restricted to

[1] These authors contributed equally to this work.
[2] Address correspondence to zhangxs@sdau.edu.cn.
The author responsible for distribution of materials integral to the findings presented in this article in accordance with the policy described in the Instructions for Authors (www.plantcell.org) is: Xian Sheng Zhang (zhangxs@sdau.edu.cn).
OPEN Articles can be viewed without a subscription.
www.plantcell.org/cgi/doi/10.1105/tpc.16.00640

the region of future *WUS* expression due to the spatiotemporal repression of cytokinin biosynthetic genes *ISOPENTENYLTRANSFERASE* (in Arabidopsis, *AtIPTs*) by AUXIN RESPONSE FACTOR3 (ARF3). Even though the importance of cytokinin and auxin in shoot regeneration is well known, the underlying molecular mechanisms remain to be elucidated. Particularly, the hormonal regulation of *WUS* expression is largely unknown.

In this study, we show that cytokinin signaling components type-B ARRs directly activate *WUS* transcription and repress the expression of auxin biosynthetic genes *YUCCAs* (*YUCs*), which in turn indirectly promotes *WUS* induction. Thus, the dual roles of type-B ARRs on *WUS* transcription are critical for activating the stem cell program during regeneration. The results of this study provide critical information for understanding the mechanism of cytokinin-regulated shoot regeneration.

RESULTS

ARR1, ARR10, and ARR12 Display Dynamic Expression Patterns during Shoot Regeneration

An Arabidopsis shoot induction system described previously was adopted for the analysis of shoot regeneration in this study (Buechel et al., 2010). First, root explants were pretreated in an auxin-rich callus induction medium (CIM) to generate callus. The callus was then transferred onto a cytokinin-rich shoot induction medium (SIM) to allow shoot induction. It has been shown that *ARR1*, *ARR10*, and *ARR12* play primary roles in transducing cytokinin signaling (Sakai et al., 2001; Ishida et al., 2008; Hill et al., 2013). Therefore, to investigate how cytokinin regulates *WUS* expression and shoot regeneration, we first traced the spatiotemporal expression patterns of the three *ARR* genes using translational reporter lines. ARR signals were hardly detectable at the beginning of SIM incubation. The signals were induced at 2 d on SIM (SIM2) and were enhanced throughout the explant at SIM4. At SIM6, ARR signals were restricted to discrete regions, wherein *WUS* signals became detectable in a few cells. At SIM8, ARR signals were restricted to the callus protuberance, colocalizing with that of *WUS*, which marks the regeneration of the stem cell niche. When the shoot meristems were established at SIM12, the signals were located in the central region of the meristem, beneath several layers of the outermost cells and overlapped with that of *WUS* (Figure 1A). The expression pattern of *ARR1* was further confirmed using the transcriptional reporter line and in situ hybridization (Supplemental Figure 1). These results suggest that ARR1, ARR10, and ARR12 function locally in shoot regeneration.

Reestablishment of Shoot Meristem Requires the Function of *ARR1*, *ARR10*, and *ARR12*

Previous studies showed that shoot regeneration capacity was impaired in the *arr1* single mutant, as well as its double and triple mutants with *arr10* and *arr12*, indicating that type-B ARRs, which are key regulators in cytokinin signaling, are required for shoot regeneration in Arabidopsis (Ishida et al., 2008; Hill et al., 2013). To determine the roles of ARR in the regeneration of shoots in callus on SIM, the transcription of *ARR1*, *ARR10*, and *ARR12* needs to be temporally repressed. For this purpose, we used artificial microRNAs (am) driven by an ethanol-inducible promoter to silence the transcripts of *ARR1*, *ARR1/10*, *ARR1/12*, *ARR10/12*, or *ARR1/10/12* (*am-ARR1*, *am-ARR1/10*, *am-ARR1/12*, *am-ARR10/12*, and *am-ARR1/10/12*, respectively) (Leibfried et al., 2005; Zhao et al., 2010). The efficiency and specification of these artificial microRNAs were tested by real-time PCR. The results demonstrate that within 12 h of ethanol induction, the transcript levels of the corresponding target *ARRs* in different transgenic lines were significantly reduced, whereas those of other type-B *ARRs*, including *ARR2*, *ARR11*, *ARR13*, *ARR18*, and *ARR21* as controls, were not obviously affected (Supplemental Figure 2).

In the wild type, the regenerated shoots in callus were identified at SIM12, and the frequency peaked at SIM22. Under ethanol treatment, regenerated wild-type shoots were observed at SIM14 and reached the peak frequency of regeneration at SIM24 (86.61%) (Supplemental Figure 3), indicating that ethanol has little effect on shoot induction. By contrast, shoot regeneration capacity in the callus expressing artificial microRNAs of *ARRs* was obviously impaired. Although the *am-ARR1* lines showed a slightly reduced regeneration frequency, the *am-ARR1/10*, *am-ARR1/12*, or *am-ARR10/12* lines gave rise to roots, and shoot regeneration was significantly inhibited. The *am-ARR1/10/12* lines showed a more severe phenotype (Supplemental Figure 3).

To further dissect the function of *ARR1*, *ARR10*, and *ARR12*, we silenced their transcription at different stages during shoot formation. As a result, ethanol induction started before restricted *WUS* expression at SIM4 largely abolished shoot regeneration (frequency of shoot regeneration, 33.18%); instead, roots were regenerated after prolonged incubation (Figures 1B and 1C). However, when ethanol induction was started after the specification of shoot stem cell niche at SIM8 or the establishment of the shoot meristem at SIM12, the percentages of shoot regeneration at SIM8 (77.24%) and SIM12 (81.84%) were similar to those of the nontreated control (85.98%) (Figures 1B and 1C). Once the shoot meristem is determined, low levels of *ARR1*, *ARR10*, and *ARR12* transcripts are enough to maintain shoot development.

ARR1, *ARR10*, and *ARR12* Control Shoot Regeneration through Regulating *WUS* Expression

Overlapping expression of ARRs and *WUS* prompted us to test whether *ARRs* regulate *WUS* transcription. We first detected the transcript levels of *WUS* during shoot regeneration using RT-qPCR and found an obvious reduction in the *arr1 10*, *arr1 12*, and *arr10 12* double mutants (Figure 2A). We further visualized the expression pattern of *WUS* using *gWUS-GFP*$_3$ reporter lines (Tucker et al., 2008). In control lines, under ethanol treatment, GFP signals were detected and restricted to the callus protuberance in 27.50% callus at SIM10. At SIM14, the signals were observed in the OC of regenerated shoot meristem at a frequency of 31.77% (Figure 2B). However, in the *am-ARR10/12* transgenic lines, *gWUS-GFP*$_3$ signals diminished and shoot meristem formation was abolished in some examined callus. At SIM10 and SIM14, GFP signals were detected in 13.75 and 17.44% of the callus, respectively, but the signals were largely reduced compared with those in control lines. These results indicate that *ARR1*, *ARR10*, and *ARR12* positively regulate the transcription of *WUS* (Figure 2B).

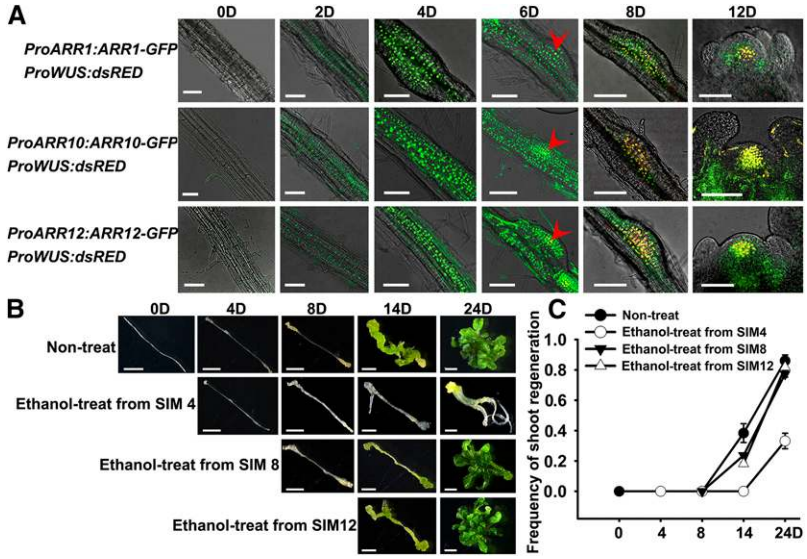

Figure 1. *ARR1*, *ARR10*, and *ARR12* Function Locally in Shoot Regeneration Following Callus Induction.

(A) Expression patterns of *ProARR1:ARR1-GFP*, *ProARR10:ARR10-GFP*, and *ProARR12:ARR12-GFP* reporters (green). *WUS* signal is indicated by a *ProWUS:dsRED* reporter (yellow). *WUS* signal became detectable at SIM6 (red arrowheads). Bars = 100 μm.

(B) Silencing of *ARR1*, *ARR10*, and *ARR12* before *WUS* expression was restricted at SIM4 severely inhibited shoot regeneration, while silencing of these genes after the specification of the shoot stem cell niche at SIM8 or the establishment of the shoot meristem at SIM12 resulted in a shoot regeneration percentage similar to that of the nontreated control. Bars = 2 mm.

(C) Shoot regeneration frequencies of **(B)**. Error bars indicate the standard deviations of three biological replicates. For each replicate, more than 100 individual plants were used. Days after the callus was transferred onto SIM are indicated by "D."

To confirm the regulatory roles of ARRs on *WUS* during shoot regeneration, we performed a 24-h ethanol induction at days 0, 4, 8, and 12 of SIM incubation, respectively, and visualized the expression pattern of *gWUS-GFP*$_3$ signals. The results show that restricted *WUS* expression was visible at SIM8 and SIM12 in the nontreated wild type, ethanol-treated wild type, and nontreated *am-ARR1/10/12* line (Figure 3); however, silencing of *ARR1*, *ARR10*, and *ARR12* obviously reduced *WUS* expression signals (Figure 3). Additionally, RT-qPCR analysis confirmed that a 24-h ethanol treatment significantly reduced the transcript levels of *WUS* at SIM8 and SIM12 in the *am-ARR1/10/12* lines, respectively (Figure 2C).

We next examined whether the regulation of ARRs on *WUS* is involved in shoot regeneration. For this purpose, we overexpressed *WUS* in the *arr1 12* double mutant and examined the regenerative capacity. All of the examined *Pro35S:WUS arr1 12* lines reached 100% of shoot regeneration, indicating that *WUS* expression is sufficient to rescue the shoot regeneration defects caused by *ARR* mutations (Figure 4). These results together demonstrate that *ARR1*, *ARR10*, and *ARR12* are involved in shoot regeneration through regulating *WUS* expression.

ARR1, ARR10, and ARR12 Directly Activate *WUS* Transcription

To test whether the activation of ARRs on *WUS* transcription is direct, we performed chromatin immunoprecipitation (ChIP) analyses. As a result, three fragments (WUS-2, WUS-3, and WUS-4) containing B-type ARR binding element sites in the *WUS* promoter were strongly enriched at SIM4, SIM8, and SIM12 (Figure 5A). The direct binding of ARRs to the ChIP-positive fragments was examined by electrophoretic mobility shift assays (EMSAs). Two oligonucleotides designated as "Probe a" (−414 to −473 bp upstream of the ATG start codon) and "Probe b" (−559 to −611 bp upstream of the ATG start codon) were biotin labeled. All three ARRs produced clear band shifts with both of these probes (Figure 5B). Moreover, the addition of excess unlabeled competitor probes effectively reduced the amount of shifted bands, indicating that ARR proteins bind specifically to the tested probes. Direct binding was also confirmed by yeast one-hybrid analyses (Figure 5C).

Moreover, the effects of ARR1, ARR10, or ARR12 on the expression of *LUC* driven by *WUS* promoter were examined in a protoplast transient expression system. The results showed that coexpression of *ARR1*, *ARR10*, or *ARR12* significantly enhanced *ProWUS:LUC* activity (Figure 5D). The activation of *WUS* transcription by ARR1, ARR10, and ARR12 was further confirmed using a transient expression assay in tobacco (*Nicotiana benthamiana*) leaves (Supplemental Figure 4). These results indicate that ARR1, ARR10, and ARR12 activate *WUS* transcription by directly binding to its promoter region.

We next determined whether the ARR binding elements on the *WUS* promoter contribute to transcriptional regulation during shoot regeneration. For this purpose, we specifically disrupted ARR binding elements within the ChIP-positive fragments (Figure 5A) and examined the transcriptional activation of ARR through a transient expression assay in tobacco leaves. We generated *ProWUSm*$_1$ by mutating the two most important base pairs

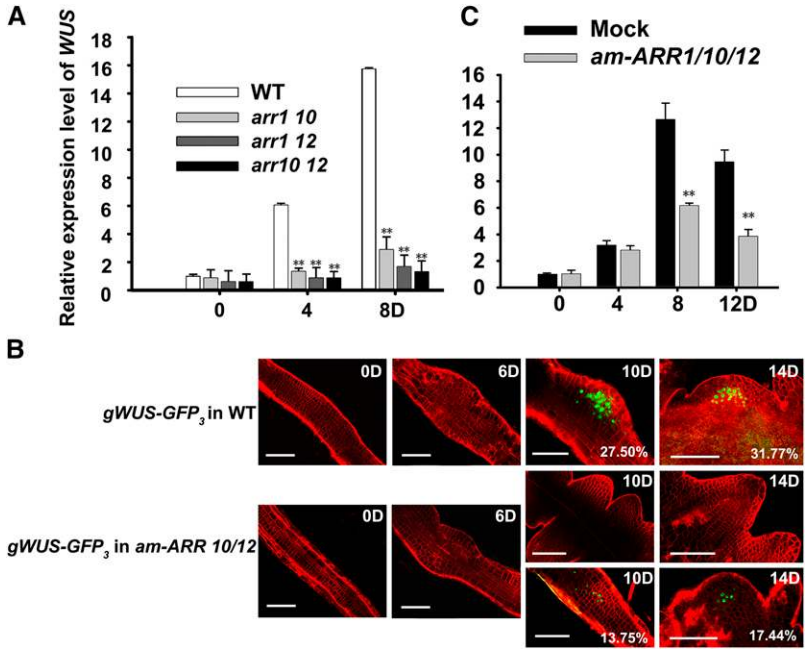

Figure 2. Defects in *ARR1*, *ARR10*, and *ARR12* Reduce *WUS* Expression.

(A) Relative transcript levels of *WUS* in the *arr1 10*, *arr1 12*, and *arr10 12* double mutants during shoot regeneration were detected by RT-qPCR.
(B) Expression of *gWUS-GFP*$_3$ (green) in wild-type and *am-ARR10/12* transgenic lines. Ethanol induction was started at the beginning of SIM incubation. Cell outlines are marked by FM4-64 (red). For *am-ARR10/12* transgenic lines at 10 and 14 d after SIM incubation, regeneration of both the root (upper) and the shoot (lower) is shown. Numbers in the lower right corner indicate the percentage of callus exhibiting the expression pattern. Bars = 50 μm.
(C) A 24-h ethanol induction was performed on *am-ARR1/10/12* callus at days 0, 4, 8, and 12 of SIM incubation, respectively. Transcript levels of *WUS* were then detected by RT-qPCR. Mock represents nontreated control. For **(A)** and **(C)**, error bars represent standard deviations of three biological replicates. Asterisks denote significant difference compared with control, as determined by a Student's *t* test, with two asterisks denoting $P < 0.01$. Days after the callus was transferred onto SIM are indicated by "D."

(GATC/T to CTTC/T) in all of the ARR binding elements of WUS-2, WUS-3, and WUS-4 (Sakai et al., 2000). As a result, the transcriptional activation was significantly reduced (Supplemental Figures 5A and 5B). WUS-3 (−706 to −396 bp upstream of the ATG start codon) largely overlapped with the previously identified region (−726 to −541 bp upstream of the ATG start codon), which is necessary for the proper expression of *WUS* (Bäurle and Laux, 2005) (Supplemental Figures 5A and 5B). We thus generated the *ProWUSm*$_2$ promoter by mutating the 2 bp of ARR binding elements in WUS-3, which demonstrated a similar result with that of *ProWUSm*$_1$ (Supplemental Figures 5A and 5B). The results indicate that ARR binding elements within WUS-3 played primary roles in ARR-mediated *WUS* transcription.

We then asked whether a 1-bp mutation is sufficient to disrupt ARR-mediated activation. To confirm this, we generated *ProWUSm*$_3$ (GATC/T to CATC/T) and *ProWUSm*$_4$ (GATC/T to GTTC/T) by mutating 1 bp of ARR binding elements in WUS-3. The transcriptional activation by ARR was partially repressed (Supplemental Figures 5A and 5B).

The *ProWUSm*$_2$ promoter was then used to drive a GFP reporter, and the signals were examined at different stages of SIM incubation. Compared with those of *ProWUS:GFP*$_3$ and in situ hybridization, *ProWUSm*$_2$*:GFP*$_3$ signals were obviously reduced during the SIM incubation (Supplemental Figures 5C and 5D). These results indicate that the ARR binding elements are required for proper expression of *WUS* during SAM formation.

The Integrated Functions of ARRs Confer the Proper Expression Patterns of *YUC1* and *YUC4*

Our previous work showed that during shoot regeneration, auxin response signals could not be detected in the *WUS*-expressing region, where cytokinin responses are strong (Cheng et al., 2013). We thus speculated that auxin accumulation was repressed by cytokinin signaling in this region. To test this hypothesis, we examined whether ARRs regulate the expression of *YUC* genes, which encode key enzymes for auxin biosynthesis. Because our previous results showed that *YUC1* and *YUC4* play essential roles in shoot regeneration, we detected the expression patterns of both of these genes (Cheng et al., 2013). Indeed, the transcript levels of *YUC1* and *YUC4*, but not *YUC2* and *YUC6*, were obviously increased in *arr1 10*, *arr1 12*, and *arr10 12* double mutants compared with those in their wild-type counterparts (Figure 6A). Therefore, *ARR1*, *ARR10*, and *ARR12* negatively regulate *YUC1* and *YUC4* transcription.

To further dissect the regulation of ARRs on *YUC* genes, we examined the expression patterns of *YUC4* and *ARR10* using double reporter lines during shoot regeneration (Figure 6B). At the

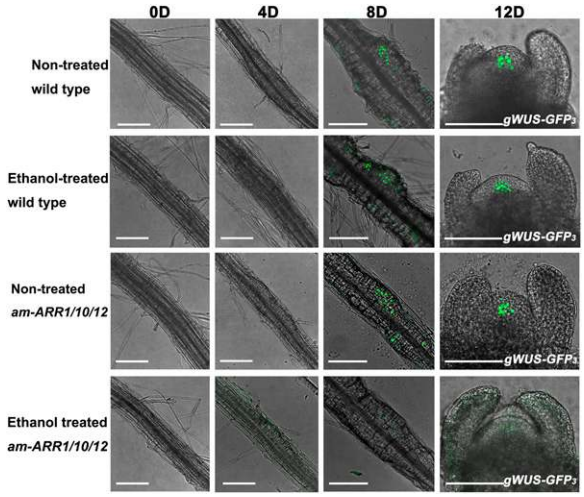

Figure 3. Inducible Silencing of *ARR1*, *ARR10*, and *ARR12* Attenuates *WUS* Expression.

A 24-h ethanol induction was performed on wild-type or *am-ARR1/10/12* callus at days 0, 4, 8, and 12 of SIM incubation, respectively. The expression of *gWUS-GFP*$_3$ was examined afterwards. Bars = 100 μm.

early stages of SIM incubation (SIM2 and SIM4), the distribution patterns of YUC4 were similar to those of ARR10, although its signals were weaker than those of ARR10. When ARR10 signals were regionalized, YUC4 signals were substantially decreased in the ARR-expressing regions at SIM6 and were further reduced at SIM8. At SIM12, YUC4 signals were undetectable in the center region of the shoot meristem where *ARR10* was expressed.

We further compared the spatiotemporal expression patterns of a *ProYUC4:YUC4-GFP* reporter in the wild type and *arr10 12* double mutant explants. In the wild-type explants, GFP signals were progressively confined to a pattern apical and peripheral to the *WUS*-accumulating region, which was initiated in the region with weak GFP signals at SIM6. When a shoot meristem was formed, YUC4 signals were switched to the region apical to the *WUS*-expressing area, as previously described (Figure 6C) (Cheng et al., 2013). However, much stronger signals in the *arr10 12* double mutant were observed at 0 and 4 d on SIM than in the wild type (Figure 6C). At SIM8, the expression pattern of *YUC4* was abolished, and *WUS* expression was not detected. Instead, the GFP signals were still evenly distributed in the explants and accumulated in the root apical meristem (Figure 6C). At SIM12, strong GFP signals accumulated in the root meristem (Figure 6C). The expression patterns of *YUC4* in the *arr10 12* double mutant were further confirmed by *ProYUC4:GUS* expression analysis (Supplemental Figure 6A). Expression of *YUC1* in the *arr1 10* and *arr1 12* double mutants also showed similar patterns to those of *YUC4* in the *arr10 12* double mutant (Supplemental Figure 6B). Finally, we examined the auxin response in the *arr10 12* double mutant using *ProDR5:GFP*. As expected, GFP signals in the *arr10 12* double mutant transgenically expressing *ProDR5:GFP* exhibited patterns similar to those of *YUC1* and *YUC4* (Figure 6C). Thus, the results suggest that ARR1, ARR10, and ARR12 repress the expression of *YUC1* and *YUC4* in the region destined for OC specification, thus restricting the expression of *YUC1* and *YUC4* to the surrounding region.

Spatiotemporal Expression of *YUC1* and *YUC4* Mediated by Type-B ARRs Is Required for Shoot Regeneration

To further test whether the spatiotemporal regulation of *YUC* expression is required for shoot regeneration, we analyzed the shoot regeneration capacity in the dominant gain-of-function *yuc1* mutant (*yuc1D*) and the *YUC4*-overexpressing transgenic lines (*YUC4ox*) (Zhao et al., 2001; Cheng et al., 2006). The *yuc1D* and *YUC4ox* explants exhibited phenotypes similar to those of the double mutants of *arr1*, *arr10*, and *arr12*, i.e., attenuated shoot regeneration and enhanced adventitious root formation (Figures 7A and 7B). Consistently, the transcript levels of *WUS* were markedly reduced in transgenic lines overexpressing *YUC1* or *YUC4* (Supplemental Figure 7A). Furthermore, we detected auxin responses of *YUC4ox* using a *ProDR5:GFP* reporter. The GFP signals were spread into the whole explant, suggesting that the locally synthesized auxin functions in a cell-autonomous manner (Supplemental Figure 8).

We examined the shoot regeneration capacity of the *yuc1 4* double mutant, and the results showed that explants of the *yuc 1 4* double mutant gave rise to filaceous structures and reduced shoots (Supplemental Figures 9A and 9B). The *arr10 12 yuc1 4* quadruple mutant exhibited similar phenotypes to that of the *yuc1 4* double mutant (Supplemental Figures 9A and 9B). Comparison of the transcript levels of *ARR10* and *ARR12* in the wild type and

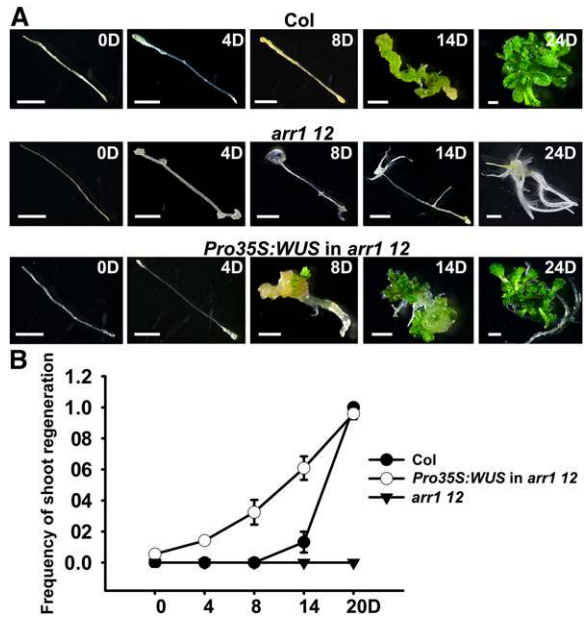

Figure 4. Overexpressing *WUS* Is Sufficient to Rescue the Shoot Regeneration Defects in the *arr1 12* Double Mutant.

(A) Shoot regeneration defects were rescued in the *Pro35S:WUS arr1 12* lines. Bars = 2 mm.

(B) Shoot regeneration frequencies of **(A)**. Error bars indicate the standard deviations of three biological replicates. For each replicate, more than 100 individuals were used. Days after the callus was transferred onto SIM are indicated by "D."

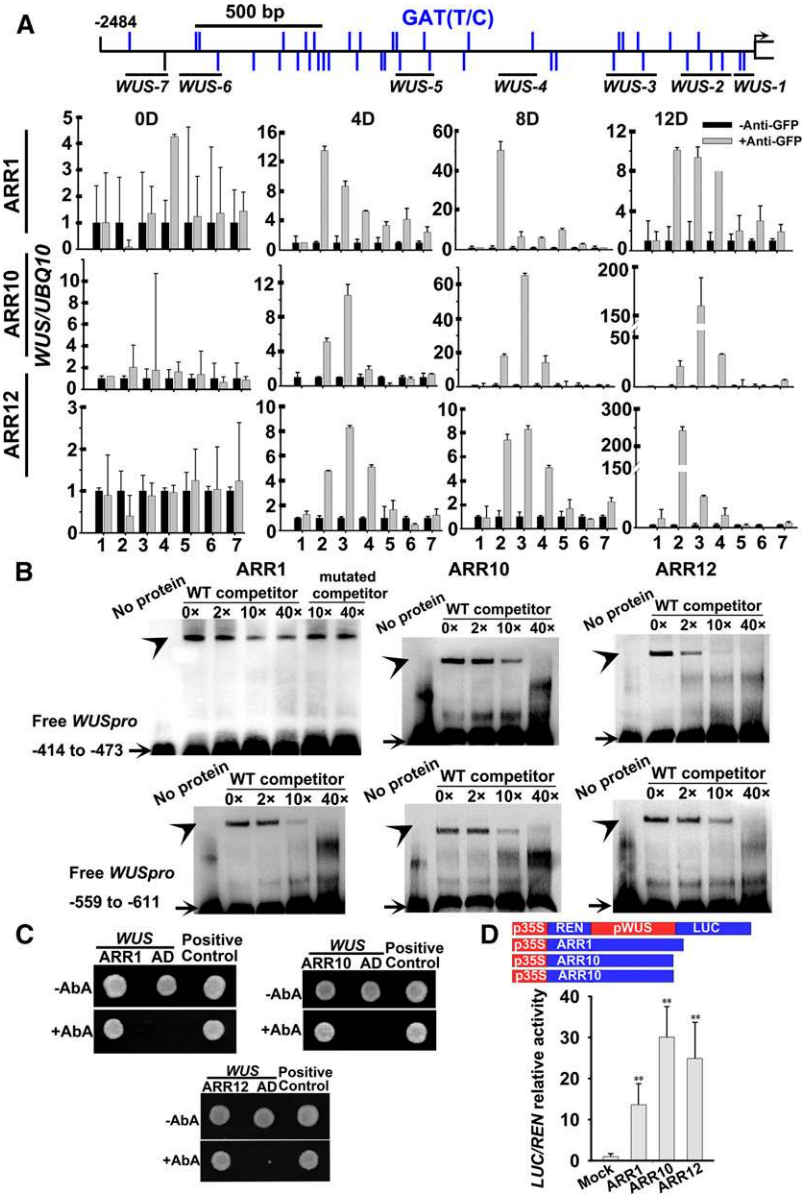

Figure 5. ARR1, ARR10, and ARR12 Directly Activate *WUS* Transcription.

(A) ChIP analyses show that ARR1, ARR10, and ARR12 bind the promoter of *WUS*. Scheme of the promoter regions of *WUS* are shown on the top. WUS-1 to WUS-7 indicate the positions of the fragments used for the ChIP-qPCR analyses. The blue bars indicate the type-B ARR binding elements GAT(T/C). "-2484" on the left indicates 2484 bp upstream of the ATG start codon. The arrow on the left represents the position of the ATG start codon. Days after the callus was transferred onto SIM are marked by "D."

(B) EMSAs confirm that ARR1, ARR10, and ARR12 associate with the *WUS* promoter region. Upper panels: Probe a (−414 to −473 bp upstream of the ATG start codon). Lower panels: Probe b (−559 to −611 bp upstream of the ATG start codon). Arrowheads indicate band shifts (complexes of ARR protein and probe DNA). Arrows indicate free probe. Nonlabeled oligonucleotides were used as competitors. Mutated competitors were generated by replacing 2 bp in the ARR binding elements (GATC/T to CTTC/T).

(C) Yeast one-hybrid assays demonstrate that ARR1, ARR10, and ARR12 associate with *WUS* promoter regions.

(D) ARR1, ARR10, or ARR12 significantly enhanced *ProWUS:LUC* activity in a protoplast transient expression system. Asterisks denote significant difference compared with the control, as determined by a Student's *t* test, with two asterisks denoting $P < 0.01$. Error bars in **(A)** and **(D)** represent standard deviations of three biological replicates.

those in *yuc1D* and *YUC4ox* using RT-qPCR did not reveal any obvious differences (Supplemental Figure 9C). These results suggest that *YUCs* act downstream of the type-B *ARRs*.

Next, we investigated whether suppression of *YUCs* in the expressing domains of type-B *ARRs* is essential for shoot regeneration. We generated transgenic lines expressing *YUC4* driven

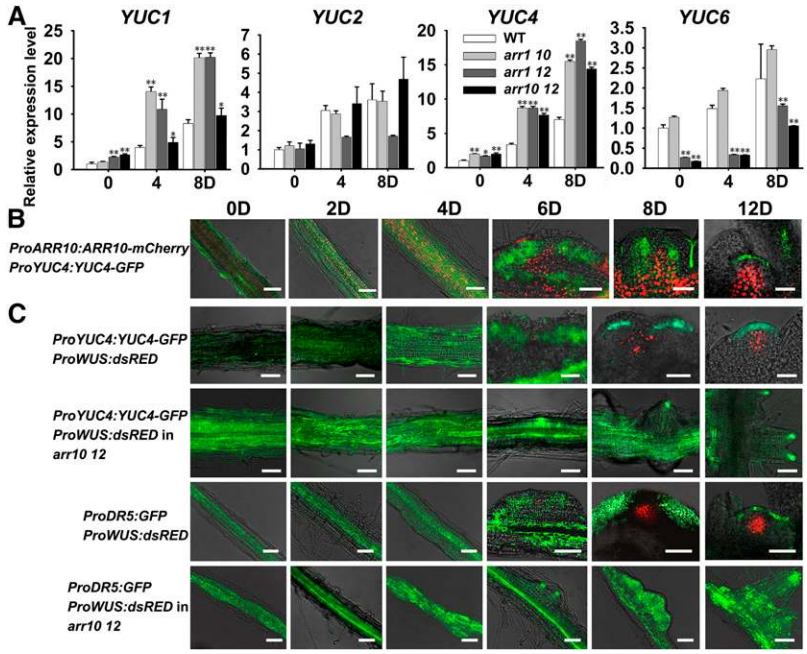

Figure 6. ARR1, ARR10, and ARR12 Negatively Regulate the Expression of *YUCs* during Shoot Regeneration.

(A) Relative transcript levels of the *YUC* genes in the *arr1 10*, *arr1 12*, and *arr10 12* double mutants were detected by RT-qPCR. Error bars represent standard deviations of three biological replicates. Asterisks denote significant difference compared with the wild-type callus, as determined by Student's *t* test, with two asterisks and one asterisk denoting $P < 0.01$ and $P < 0.05$, respectively.

(B) Distribution of signal derived from *ProARR10:ARR10-mCherry* (red) and *ProYUC4:YUC4-GFP* (green) during shoot regeneration.

(C) Expression patterns of *ProYUC4:YUC4-GFP* (green), *ProDR5:GFP* (green), and *ProWUS:dsRED* (red) reporters in the wild type and *arr10 12* double mutants during shoot regeneration. Days after the callus was transferred onto SIM were marked by "D." Bars = 50 μm.

by the promoter of *ARR10* and examined their capacity for shoot regeneration. Compared with those of the wild-type explants, the frequencies of shoot regeneration in *ProARR10:YUC4* lines were obviously decreased (Figures 7A and 7C), indicating that repression of *YUC4* in the type-B *ARRs* expression domain is essential for shoot regeneration. We further determined whether repressing *YUC* expression in the *WUS*-expressing region is critical for shoot regeneration. To this end, we introduced transgenic lines expressing *YUC4* under the *WUS* promoter. Shoot regeneration in *ProWUS:YUC4* lines was severely reduced, demonstrating the importance of repressing *YUC* expression in the de novo formation of OC (Figures 7A and 7C). The results together indicate that spatial localization of *YUC* is important for shoot meristem formation.

To test whether *YUC1* and *YUC4* expression is directly regulated by ARRs, we performed ChIP assays. The results showed that ARR1, ARR10, and ARR12 associate with the YUC4-1 and YUC4-2 fragments of the *YUC4* promoter, while ARR1 also associates with the YUC1-5 region of the *YUC1* promoter in callus tissue at SIM4, SIM8, and SIM12 (Figure 8A; Supplemental Figures 7B and 7C). EMSA and yeast one-hybrid analyses revealed direct binding of the ARRs to the fragments of the *YUC4* promoter (Figures 8B and 8C). Furthermore, we generated a construct containing the *GFP* gene driven by the mutated *YUC4* promoter (*ProYUC4m*) within which 2 bp of the binding elements by ARR1, ARR10, and ARR12 were mutated (GATC/T to CTTC/T). The *ProYUC4m:GFP* signal in the wild-type background showed similar patterns to those of *ProYUC4:GFP* in the *arr10 12* double mutant (Figure 8D). Together, these results indicate that ARR1, ARR10, and ARR12 redundantly occupy *YUC* promoters and suppress their expression and thus prevent the auxin-mediated repression of *WUS* transcription.

Finally, we analyzed whether direct binding of ARRs on *YUC* promoters mediated shoot regeneration. For this purpose, we expressed *YUC4* under the mutated *YUC4* promoter (*ProYUC4m*) and examined the regeneration capacity of these transgenic lines. As a result, misexpression of *YUC4* by these promoters led to an obvious decrease in shoot regeneration percentage (Supplemental Figure 10). The results indicate that the binding elements of ARRs on *YUC* promoters are critical for shoot regeneration.

ARRs Regulate SAM Maintenance through Regulating *WUS* Transcription in Planta

To validate the above-described regulatory relationship between *WUS* and these hormone-related genes in planta, we performed experiments to visualize their expression patterns in the SAM. We first visualized the distribution patterns of ARR1, ARR10, and ARR12 in the SAM and found their signals to be located in the central region of the SAM, overlapping with the OC marked by *WUS* signals (Supplemental Figure 11A). *WUS* expression was then detected in the *arr1 10 12* mutant and the *am-ARR1/10/12* transgenic lines using the *gWUS-GFP*$_3$ reporter. GFP signals were obviously reduced in the *arr1 10 12* mutant compared with those in the wild type (Figures 9A and 9C). In the *am-ARR1/10/12* lines,

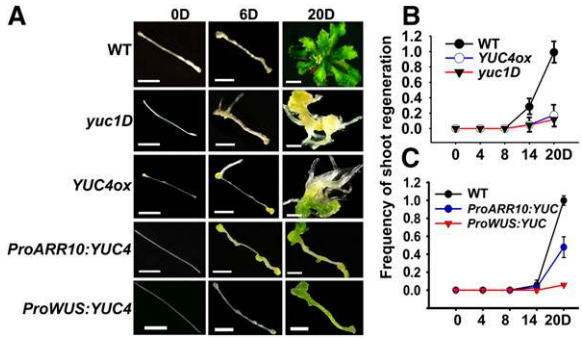

Figure 7. *YUC* Expression Is Involved in Shoot Regeneration.

(A) Shoot induction in mutant and transgenic lines with disordered expression of *YUC* genes. The number of days of SIM incubation is indicated above each column of panels. Bars = 2 mm.
(B) Shoot regeneration frequencies of *yuc1D* and *YUC4ox* lines.
(C) Shoot regeneration frequencies of *ProARR10:YUC4* and *ProWUS:YUC4* transgenic lines. For each replicate in **(B)** and **(C)**, more than 100 individuals were used. Error bars indicate the standard deviations of three biological replicates.

ethanol treatment for 24 h significantly downregulated *WUS* expression signals compared with the control lines (Figures 9B and 9C). ChIP assays revealed that ARR1, ARR10, and ARR12 associate with the *WUS* promoter, respectively (Figure 9D). Thus, three ARRs are required for maintaining *WUS* expression in the OC through their direct activation of *WUS* transcription.

We next investigated the effect of *ARR1*, *ARR10*, and *ARR12* on the expression of *YUC4* by visualizing *ProYUC4:YUC4-GFP* and *ProWUS:dsRED* reporters (Figure 10A). Signals derived from *ProYUC4:YUC-GFP* were located in the L1 cell layer of the wild-type SAM, but expanded to the central region of the SAM in both the *arr10 12* and *arr1 10 12* mutants. Also, the signals were much stronger in the *arr1 10 12* triple mutant than in the *arr10 12* double mutant (Figure 10A). By contrast, the *WUS*-expressing region was decreased in the *arr10 12* double mutant and was even less in the *arr1 10 12* triple mutant, compared with those in the wild type (Figure 10A). Furthermore, ChIP analysis revealed a direct regulation of ARR1, ARR10, and ARR12 on *YUC4* expression (Supplemental Figures 11B and 11C), suggesting that the three ARRs repress *YUC* expression and, thus, auxin accumulation in the OC, which indirectly promotes *WUS* transcription therein.

We questioned whether the regulation of *WUS* by the ARRs exerts roles in SAM maintenance. The SAM of the *arr1 10 12* triple mutant, *yuc1D*, *YUC4ox*, and *ProARR10:YUC4* lines was examined. Consistent with the reduced transcript levels of *WUS*, the SAM size of these lines was decreased compared with that of the wild type (Figures 10B and 10C; Supplemental Figure 12). The *arr1 10 12* triple mutant exhibited the greatest magnitude of reduction (Figures 10B and 10C). Further analyses demonstrated that the decrease in SAM size resulted from a reduced cell number (Figure 10C). We thus suggest that defects in *ARR1*, *ARR10*, and *ARR12* cannot activate *WUS* transcription. Furthermore, these defects caused ectopic expression of *YUC1* or *YUC4* in the OC, which might lead to auxin accumulation and subsequent *WUS* suppression. This fits well with the recent finding that *WUS* acts as a positive regulator of cell division, and inducible downregulation of *WUS* expression resulted in a progressive decrease in SAM size (Yadav et al., 2010). Thus, these results suggest that ARR1, ARR10, and ARR12 mediate SAM maintenance through their regulation of *WUS* transcription.

DISCUSSION

ARR1-, *ARR10*-, and *ARR12*-Regulated *WUS* Expression Plays Critical Roles in Shoot Regeneration

Double and triple mutants of *ARR1*, *ARR10*, and *ARR12* could not generate shoots under in vitro culture owing to cytokinin insensitivity (Hill et al., 2013; Ishida et al., 2008). Here, we used ethanol-induced artificial microRNAs to silence the transcription of *ARR1*, *ARR10*, and *ARR12* at different stages of shoot formation. As a result, the capacity of shoot regeneration was largely reduced in these lines, confirming that these ARRs control shoot regeneration (Figure 1B; Supplemental Figure 3).

A previous study demonstrated that shoot regeneration capacity was largely reduced in the *wus-1* mutant (Gordon et al., 2007). To confirm the role of WUS in shoot regeneration, we transferred the *WUS* gene driven by *Pro35S* promoter to the *arr1 12* mutant and found that overexpressing WUS is sufficient to rescue the shoot regeneration phenotype of the *arr1 12* mutant (Figure 4), suggesting that WUS functions in downstream of cytokinin signaling and plays a critical role in shoot regeneration. Since *WUS* expression is regulated by *ARR1*, *ARR10*, and *ARR12*, we propose that these ARRs control shoot regeneration through regulation of *WUS* expression.

Cytokinin has been shown to regulate the cell cycle in both cell culture and in planta (Riou-Khamlichi et al., 1999), and it might be involved in shoot formation by controlling cell proliferation. Here, our results indicate that inducible silencing of *ARR1*, *ARR10*, and *ARR12* significantly reduced shoot regeneration, although callus could be observed (Figure 1B). Overexpressing *WUS* rescued the defects of the *arr* mutants (Figure 4). Thus, ARR-mediated *WUS* expression plays a critical role in shoot regeneration, which may be independent of cell proliferation of callus.

In addition, our results indicated that *WUS* expression was firstly induced in a few callus cells and then marked the regeneration of the OC. However, this expression pattern is different from previous findings, which showed that *WUS* is broadly expressed across the callus at the early stage of SIM incubation, but restricted to the center of the shoot meristem later (Gordon et al., 2007; Kareem et al., 2015). To confirm this result, we performed in situ hybridization and found that the two reporters we used mimicked the expression pattern of *WUS* endogenous mRNA (Figure 1A; Supplemental Figures 5C and 5D).

ARR-Mediated *WUS* Transcription Requires RE1- or RE2-Specific Factors

Cytokinin signaling has been suggested to be a positional cue for *WUS* expression (Gordon et al., 2009). However, the regulatory pathways between cytokinin receptors and *WUS* remain to be elucidated. Our results revealed a shortcut, namely, that ARR1, ARR10, and ARR12 could directly bind to the *WUS* promoter and activate its transcription (Figure 5). A previous study analyzed the

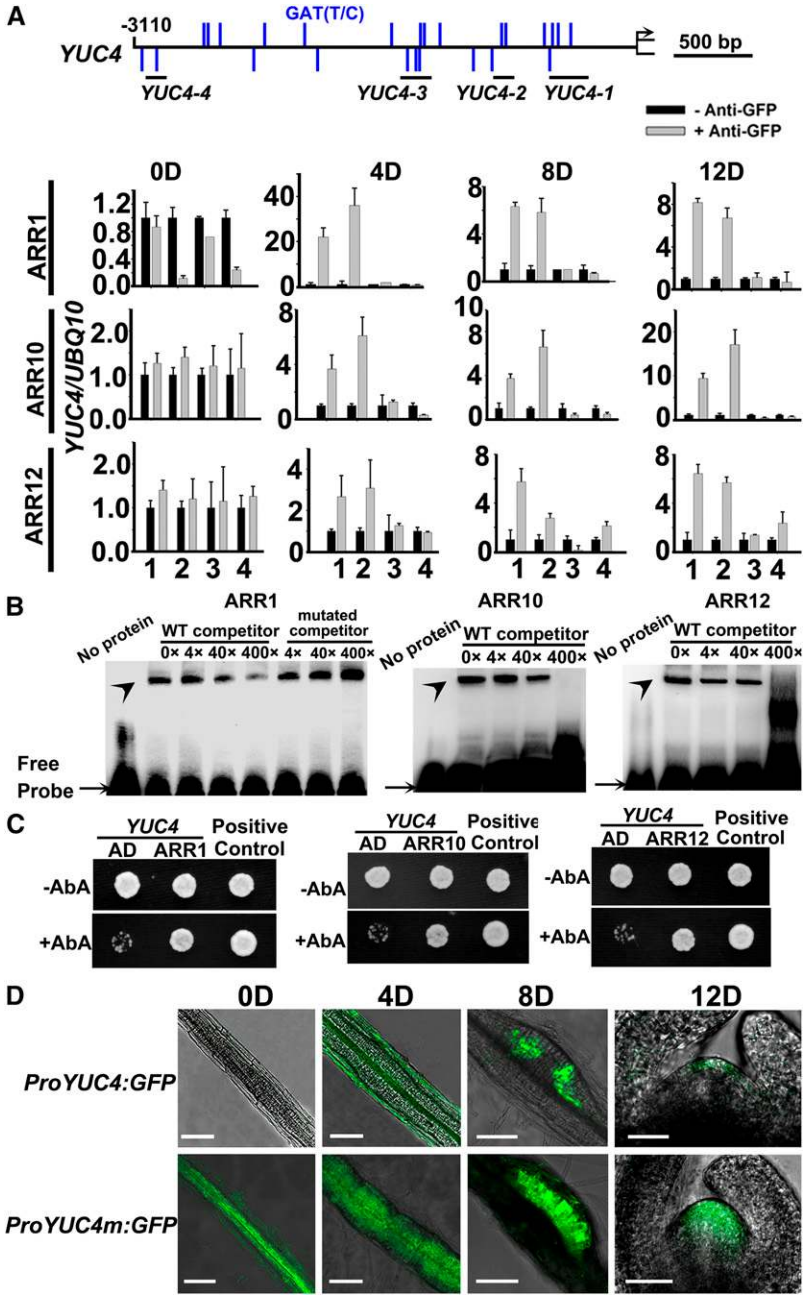

Figure 8. ARR1, ARR10, and ARR12 Bind the Promoter of *YUC4* and Repress Its Expression.

(A) ChIP analyses indicate that ARR1, ARR10, and ARR12 bind the promoter of *YUC4*. Scheme of the promoter regions of *YUC4* are shown on the top. The blue bars indicate the type-B ARR binding elements GAT(T/C). "-3110" on the left indicates 3110 bp upstream of the ATG start codon. The arrow on the left represents the position of the ATG start codon. Error bars represent standard deviations of three biological replicates.

(B) EMSAs revealed the direct association of ARR1, ARR10, and ARR12 to the *YUC4* promoter. Arrowheads indicate band shifts. Arrows indicate the free probes. Nonlabeled oligonucleotides were used as competitors. Mutated competitors were generated by replacing 2 bp in the ARR binding elements (GATC/T to CTTC/T).

(C) Yeast one-hybrid assays show that ARR1, ARR10, and ARR12 associate with the *YUC4* promoter region.

(D) Expression patterns of *ProYUC4:GFP* and *ProYUC4m:GFP*. Days after the callus was transferred onto SIM are indicated by "D." Bars = 50 μm.

regulatory roles of different regions in the *WUS* promoter and revealed that the sequences between −726 and −541 bp upstream of the start codon (−600 to −415 bp upstream of the putative transcription start site) are necessary for *WUS* expression in the stem cell niche of the inflorescence meristem (Bäurle and Laux, 2005). Here, we identified a ChIP-positive fragment (WUS-3,

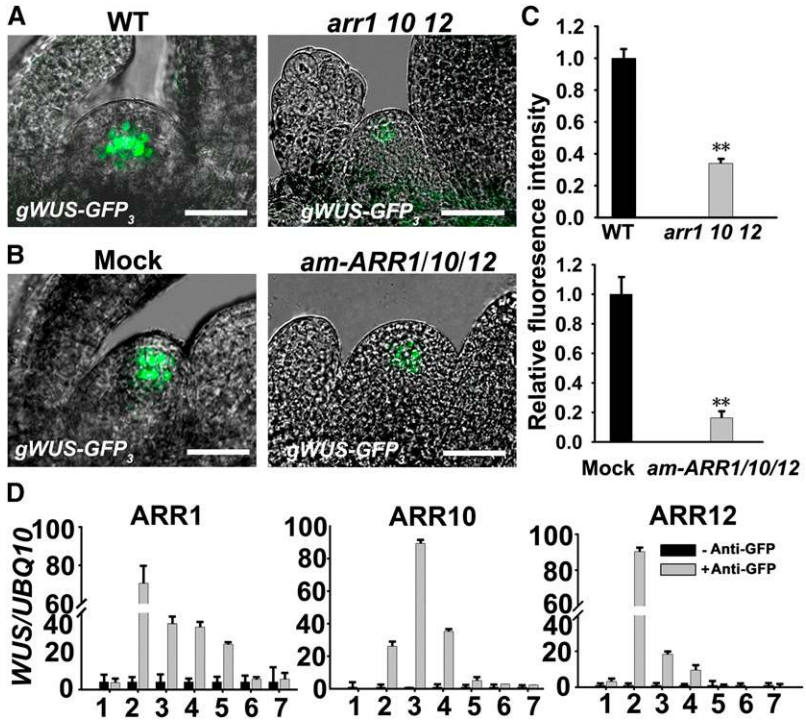

Figure 9. ARR1, ARR10, and ARR12 Activate *WUS* Transcription in the SAM.

(A) Expression of *gWUS-GFP*$_3$ in the *arr1 10 12* mutant. Bars = 50 μm.

(B) *gWUS-GFP*$_3$ signals were significantly downregulated in the *am-ARR1/10/12* lines at 24 h after ethanol treatment. Bars = 50 μm.

(C) The intensity of fluorescence in the *arr1 10 12* mutant (upper panel) and *am-ARR1/10/12* transgenic lines (lower panel) was measured using ImageJ software. Asterisks denote significant difference compared with wild-type or mock control, as determined by a Student's *t* test, with two asterisks denoting $P < 0.01$

(D) ChIP analysis showed that ARR1, ARR10, and ARR12 bind the *WUS* promoter. The positions of fragments in *WUS* promoters are shown in Figure 3A. Error bars represent standard deviations of three biological replicates.

−706 to −396 bp upstream of the ATG start codon) in the *WUS* promoter that largely overlapped with this necessary sequence (Figure 5A). Mutating the ARR binding elements within WUS-3 significantly reduced the transcriptional activation by ARR (Supplemental Figures 5A and 5B), indicating the important roles of this fragment in recruiting ARR proteins for transcriptional regulation.

Furthermore, tetrameric tandem repeats of a 57-bp regulatory region (−586 to −529 bp upstream of the putative transcription start site) were shown to be sufficient for providing the correct spatial *WUS* expression pattern in the stem cell niche, and this activity depends on two adjacent short motifs, RE1 and RE2 (Bäurle and Laux, 2005). According to the model envisioned by Bäurle and Laux, we propose a regulatory mechanism for ARR-mediated *WUS* transcription. In the OC or competent callus cells, ARR1, ARR10, or ARR12 protein is recruited by ARR binding elements within the WUS-3 fragment. Other elements located in WUS-2 and WUS-4 are also involved in the interaction between ARR protein and *WUS* promoter, but play redundant and minor roles. This is supported by the result that mutating ARR binding elements in WUS-3 or in all three ChIP-positive fragments reduced ARR-mediated activation to similar extents (Supplemental Figures 5A and 5B). Once ARR binds the promoter, it activates *WUS* transcription by interacting with the previously proposed RE1- or RE2-specific transcription factors. This hypothesis is supported by the fact that ARRs could interact with other proteins via the transactivation domain (Zhang et al., 2015).

ARR1, ARR10, and ARR12 Are Bifunctional Transcription Factors and Play Dual Roles in Regulating *WUS* Expression

Type-B ARRs have been demonstrated to be transcriptional activators, which directly bind to the promoter region of target genes, such as type-A ARRs, and positively regulate their expression (Hwang et al., 2012). Recent evidence revealed that ARR1 also directly regulates genes whose transcription was repressed by cytokinin (Zhang et al., 2013). Our data show that ARR1, ARR10, and ARR12 exhibit dual functions in transcription regulation and activate the transcription of *WUS* and repress that of *YUCs* within the same cell niche. WUS has previously been shown to have a similar dual function (Ikeda et al., 2009). It is possible that different partner proteins interacting with ARRs confer their functions as either transcriptional activators or repressors. Identifying and analyzing these partner proteins will facilitate our understanding of transcription factors with dual roles.

The de novo establishment of shoot meristem depends on the initiation and maintenance of *WUS* transcription. After the

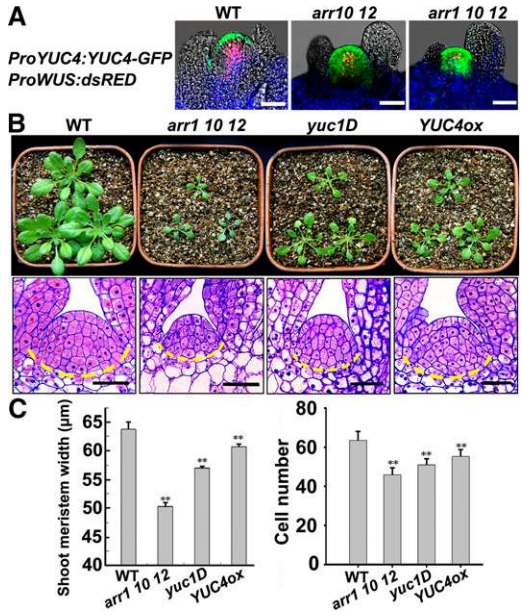

Figure 10. Spatiotemporal Expression of *YUC*s Mediated by Type-B ARRs Is Involved in SAM Maintenance.

(A) Expression patterns of *ProYUC4:GFP* (green) and *ProWUS:dsRED* (red) reporters in the wild type, *arr10 12*, and *arr1 10 12* mutants. Blue signal represents chloroplast autofluorescence. Bars = 50 μm.
(B) and **(C)** Size and cell number of the SAM in the wild type, *arr1 10 12* mutant, *yuc1D*, and transgenic lines overexpressing *YUC4*. Seedlings at 10 d after germination were used for histological analyses in **(B)**. Dashed yellow lines in **(B)** indicate the boundaries of the SAMs. Histograms in **(C)** represent width and cell number of SAMs shown in the lower panels of **(B)**. Asterisks denote significant difference compared with the wide type, as determined by a Student's *t* test, with two asterisks denoting $P < 0.01$. Bars = 50 μm.

formation of shoot meristem either from regeneration or embryonic development, proper *WUS* expression is required to maintain the stem cell niche and subsequently SAM size. Based on their dual function in transcriptional regulation, ARR1, ARR10, and ARR12 directly activated *WUS* transcription and indirectly promoted its expression by repressing auxin accumulation. Therefore, the dual regulatory roles of ARR1, ARR10, and ARR12 on *WUS* were critical for the de novo establishment of stem cell niche in vitro and were required for its maintenance in planta.

A Proposed Regulatory Network for de Novo Specification of Shoot Stem Cell Niche Controlled by Cytokinin and Auxin

Pioneer studies demonstrated that cooperation of exogenous cytokinin and auxin induces plant regeneration, which lays an important foundation for wide applications in plant biotechnology and agricultural practices (Duclercq et al., 2011; Ikeuchi et al., 2016). However, the mechanisms underlying this regeneration process are poorly understood. Combining our present results with previous findings (Cheng et al., 2013), we propose a regulatory network for shoot regeneration. During shoot induction, cytokinin signaling in the potential *WUS*-expressing region directly represses the transcription of *YUC1* and *YUC4* through type-B ARRs, thus making this region a cytokinin signaling-rich (CSR) one (Figure 11). Meanwhile, ARF3 represses the expression of *AtIPTs* in the surrounding region, giving rise to an auxin signaling-rich region in a radial pattern encircling the CSR region. Thus, antagonistic regulation between auxin and cytokinin generates the mutually exclusive distribution pattern of the two hormones. In the CSR region, cytokinin functions through ARR1, ARR10, and ARR12 activating the transcription of *WUS* and ensures a high cytokinin/auxin response ratio in this region by suppressing *YUC* expression to maintain *WUS* expression therein (Figure 11). This is supported by a recent study showing that *WUS* expression is negatively regulated by auxin signaling (Liu et al., 2014). The stable *WUS* transcription switches callus cells into OC cells, which in turn initiate stem cells through a non-cell-autonomous manner (Yadav et al., 2011; Chatfield et al., 2013; Daum et al., 2014).

Our results demonstrate that *WUS* signals were colocalized with those of *ARR1*, *ARR10*, and *ARR12* after the onset of its transcription. The expression regions of *ARR1*, *ARR10*, and *ARR12* were always larger than the *WUS* expression region (Figure 1). It is likely that other factors function together with the three ARRs to restrict *WUS* expression spatially.

It has been shown that root regeneration triggers a program similar to that of embryonic root formation (Efroni et al., 2016). However, the mechanisms underlying shoot regeneration are, at least in part, different from those of embryonic SAM establishment. During shoot regeneration, high levels of cytokinin response signals

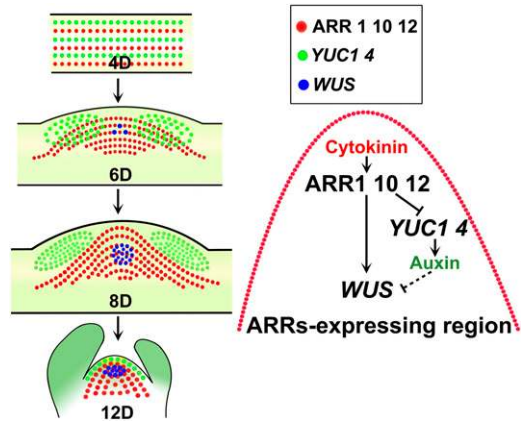

Figure 11. Dual Roles of Type-B ARRs in Regulating *WUS* Expression and Subsequent Shoot Meristem Formation.

At the early stage of shoot induction, type-B ARRs and *YUC*s were induced throughout the explant. After 6 d of incubation on SIM, the expression of *ARR1*, *ARR10*, and *ARR12* was restricted to discrete regions, wherein *YUC* signals were substantially reduced; moreover, *WUS* transcription was initiated in a few cells. When ARR signals were restricted to the callus protuberance at SIM8, *YUC* signals were further reduced there, while *WUS* signals were enhanced and detected in more cells. At SIM12, ARR1, ARR10, and ARR12 signals were enriched in the center region of the regenerated shoot meristem, where *WUS* marks the stem cell niche and *YUC* signals were undetectable. In the region of ARRs expression, the transcription of *WUS* was activated and maintained, and in parallel, auxin accumulation was inhibited by repressing the expression of *YUC*s, indirectly promoting *WUS* induction. Days after the callus was transferred onto SIM are indicated by "D."

were observed in the progenitor cells of shoot meristem before the onset of *WUS* expression. By contrast, the signals of the cytokinin response remain undetectable in the prospective SAM until the heart stage of the embryo, which is much later than the initiation of *WUS* expression (Müller and Sheen, 2008; Cheng et al., 2013; Zürcher et al., 2013). It is likely that cytokinin signaling acts upstream of *WUS* during shoot regeneration and downstream of *WUS* in embryonic SAM establishment. Consistently, our results showed that ARR1, ARR10, and ARR12 were critical for shoot regeneration but were not required for SAM formation in planta.

The de novo shoot regeneration may share similar mechanisms with axillary meristem formation. Both types of meristems are established in the region with low auxin and enriched cytokinin signaling. *ARR1* has been shown to be involved in axillary meristem initiation (Wang et al., 2014). Our results demonstrated a substantial reduction of axillary meristems in the *arr1 10 12* triple mutant (Supplemental Figure 13). It is possible that ARR1, ARR10, and ARR12 regulate axillary meristem formation through direct activation of *WUS* expression.

Mutually Exclusive Distribution Pattern of Cytokinin and Auxin Signaling Is Important for Meristem Specification

Out data show that mutually the exclusive distribution pattern of cytokinin and auxin signaling was critical for the specification of the stem cell niche during shoot regeneration. Evidence accumulated in the past few years suggests that the distinct distribution of these two hormones plays pivotal roles in tissue patterning (Chandler and Werr, 2015; Schaller et al., 2015). For instance, in the vascular tissue of Arabidopsis roots, a central localized xylem axis bisects the intervening procambium cells and thus forms a bisymmetric structure (Nieminen et al., 2015; De Rybel et al., 2016). Cytokinin signaling peaks in two bisymmetric procambial cell files, where it regulates the localization of PINFORMED (PIN) auxin efflux carriers and creates an auxin maximum in the adjacent xylem axis. Auxin signaling in turn promotes the expression of the negative regulator of cytokinin signaling *AHP6* by ARF5 (Besnard et al., 2014). This mutually exclusive pattern of cytokinin and auxin is required for the specification of the bisymmetric vascular pattern (Bishopp et al., 2011).

Moreover, when the hypophysis cell asymmetrically divides and forms the upper lens-shaped cell and the larger basal cell, the cytokinin response of the hypophysis is maintained in the former, whereas the auxin response is detected in the latter (Müller and Sheen, 2008). As a result, the lens-shaped cell gives rise to the QC and the basal cell generates the columella (Laux et al., 2004). During the initiation of the axillary meristem, an auxin minimum region in the leaf axil is established through PIN-dependent auxin efflux (Wang et al., 2014). In this region, cytokinin perception and signaling are activated to promote the formation of the functional shoot meristem, possibly through inducing *WUS* expression.

Thus, the mutually exclusive distribution of cytokinin and auxin is widely involved in the specification and function of plant meristems, which might result from the fundamental roles of these two hormones in determining cell fate (Chandler and Werr, 2015). Our study reveals that an interaction between cytokinin and auxin controls shoot regeneration through activating *WUS* expression, suggesting that inducing the expression of key regulatory genes is critical for cell fate determination.

METHODS

Plant Materials and Growth Conditions

Arabidopsis thaliana ecotype Col-0 was used as the wild type in this study except when stated otherwise. Surface-sterilized seeds were plated on half-strength Murashige and Skoog medium containing 0.8% (w/v) agar and 1% (w/v) sucrose (pH 5.7). After vernalization at 4°C for 4 d, seedlings were grown under sterile conditions or in soil at 20 to 22°C, with 16 h of white light (100 μmol m^{-2} s^{-1}) and 8 h of dark. The *ProWUS:dsRED* reporter lines were kindly provided by Elliot M. Meyerowitz (California Institute of Technology) (Gordon et al., 2007). The *gWUS-GFP*$_3$ reporter lines were kindly provided by Thomas Laux (University of Freiburg) (Zhang et al., 2013). The *arr1 10* double (CS39990), *arr1 12* double (CS6981), *arr10 12* double (CS39991), and *arr1 10 12* triple (CS39992) mutants were obtained from the ABRC. The *yuc1D* and *yuc1 4* double mutants were kindly provided by Yunde Zhao (University of California at San Diego) (Cheng et al., 2006; Zhao et al., 2001). The *arr10 12 yuc1 4* quadruple mutant was obtained by crossing *arr10 12* with *yuc1 4* double mutants.

Plasmid Construction and Plant Transformation

Artificial microRNAs targeting *ARR1*, *ARR1/10*, *ARR10/12*, and *ARR1/10/12* were designed using the WMD3-Designer and were cloned into an ethanol-inducible vector (Leibfried et al., 2005; Zhao et al., 2010) to produce the *ProAlcA:am-ARR1*, *ProAlcA:am-ARR1/10*, *ProAlcA:am-ARR1/12*, *ProAlcA:am-ARR10/12*, and *ProAlcA:am-ARR1/10/12* constructs. A genomic fragment of 4597 bp containing a 2527-bp sequence upstream of the ATG start codon and the coding region without the stop codon of *ARR1* was amplified by PCR from Arabidopsis genomic DNA with the primers pARR1-genomic-F, pARR1-genomic-R, ARR1-cDNA-F, and ARR1-cDNA-R and was recombined into pROKII-GFP to generate the *ProARR1:ARR1-GFP* expression vector. A 4953-bp genomic fragment containing a 2479-bp region upstream of the ATG start codon and the coding region without the stop codon of *ARR10* was PCR amplified using the primers ARR10-genomic-F and ARR10-genomic-R and was recombined into pMDC107 to generate the *ProARR10:ARR10-GFP* expression vector. The same genomic fragment was amplified with the primers pARR10-mCherry-F and pARR10-mCherry-R and was inserted into a p2300-H2B-mCherry vector digested with *Sac*I and *Kpn*I to generate the *ProARR10:ARR10-mCherry* vector. A genomic fragment of 5127 bp containing a 2658-bp sequence upstream of the ATG start codon and the coding region without the stop codon of *ARR12* was amplified by PCR with the primers ARR12-genomic-F and ARR12-genomic-R and was recombined into pMDC107 to generate the *ProARR12:ARR12-GFP* expression vector.

For *Pro35S:WUS*, the 879-bp coding sequence of *WUS* was amplified by PCR with the primers WUS-CDS-F and WUS-CDS-R and then inserted into the pROKII-GFP vector. For the *ProARR10:YUC4* construct, a fragment of 2479 bp upstream of the ATG start codon of *ARR10* was amplified from the Arabidopsis genomic DNA with primers pARR10-P-F and pARR10-P-R and inserted into the pCambia1300 vector digested with *Sac*I and *Bam*HI to produce pCambia1300-pARR10. The full coding sequence of *YUC4* was amplified by RT-PCR using total RNA isolated from Arabidopsis seedlings with primers YUC4-cDNA-F and YUC4-cDNA-R and inserted into pCambia1300-pARR10 digested with *Nco*I and *Sal*I. All of the expression vectors described above were transformed into the Col-0 wild type using the floral dip method. *ProYUC4:YUC4-GFP* was described previously (Cheng et al., 2013). *ProYUC4:YUC4-GFP* was transformed into wild-type plants and these plants were then crossed with *ProWUS:dsRED* lines to generate *ProYUC4:YUC4-GFP; ProWUS:dsRED* reporter lines, which were then crossed with the *arr10 12* double mutants. The *ProDR5:GFP* and *ProWUS:DsRed* reporter lines were described previously (Cheng et al., 2013) and were crossed with *arr10 12* double mutants. The

ProARR10:ARR10-mCherry lines were crossed with the *ProYUC4:YUC4-GFP* lines to generate the double reporter lines.

A 2484-bp fragment upstream of the *WUS* start codon was amplified by PCR from Arabidopsis genomic DNA (ecotype Wassilewskija) with primers pWUS-F and pWUS-R and was introduced into the pGK-3EGFP vector to generate *ProWUS:GFP*$_3$. Mutated *WUS* promoters were synthesized by Shanghai Sangon Biotechnology Incorporation (Shanghai, China). For *ProWUSm*$_1$, 2 bp of the ARR binding elements in the ChIP-positive fragments WUS-2, WUS-3, and WUS-4 were replaced (GATC/T changed to CTTC/T). For *ProWUSm*$_2$, 2 bp of the ARR binding elements in WUS-3 were replaced (GATC/T changed to CTTC/T). For *ProWUSm*$_3$, 1 bp of the ARR binding elements in WUS-3 was replaced (GATC/T changed to CATC/T). For *ProWUSm*$_4$, 1 bp of the ARR binding elements in WUS-3 was replaced (GATC/T changed to GTTC/T). *ProWUSm*$_2$ was then cloned into the pGK-3EGFP vector to generate *ProWUSm*$_2$*:GFP*$_3$. *ProWUSm*$_2$*:GFP*$_3$ and *ProWUS:GFP*$_3$ were examined in the Wassilewskija ecotype background. The *ProYUC4m* promoter was synthesized by replacing 2 bp of the ARR binding elements in YUC4-1 and YUC4-2 ChIP-positive fragments (GATC/T changed to CTTC/T). *ProYUC4m* was then cloned into pMDC107 to generate *ProYUC4m:GFP*. The coding sequence of *YUC4* was amplified by PCR using total RNA from Arabidopsis seedlings with primers YUC4-cDNA-F and YUC4-cDNA-R and was introduced into a pROKII-GFP vector to generate pROKII-YUC4-GFP. *ProYUC4m* was amplified by PCR with primers pYUC4-F and pYUC4-R and was introduced into pROKII-YUC4-GFP to generate the *ProYUC4m:YUC4* vector. To analyze the auxin response, *ProDR5:GFP* reporter lines were crossed with *YUC4ox* transgenic lines. To analyze the auxin response, *ProDR5:GFP* reporter lines were crossed with *YUC4ox* transgenic lines. The sequences of all primers are listed in Supplemental Data Set 1. The sequences of mutated promoters are listed in Supplemental Data Set 2.

The *ProARR1:GUS* transgenic line was obtained from the ABRC (Mason et al., 2004). The *Pro35S:YUC4* (*YUC4ox*), *ProYUC1:GUS*, and *ProYUC4:GUS* transgenic lines were kindly provided by Yun de Zhao (University of California at San Diego) (Cheng et al., 2006). The *ProYUC1:GUS* transgenic lines were crossed with the *arr1 10* and *arr1 12* double mutants. The *ProYUC4:GUS* lines were crossed with the *arr10 12* double mutants.

Shoot Regeneration Analysis

Plants were grown for 15 d under sterile conditions as described above. Root explants were cut at 5 to 10 mm from the root tip and incubated on CIM, containing Gamborg's B5 medium with 2% glucose, 0.5 g/L MES, 0.2 μM kinetin, 2.2 μM 2,4-D, and 0.8% agar. After 6 d in culture on CIM, explants were transferred onto SIM containing Gamborg's B5 medium with 2% glucose, 0.5 g/L MES, 0.9 μM 3-indoleacetic acid, and 5 μM 2-isopentenyladenine for shoot induction.

For ethanol induction, ethanol was added to the SIM to a final concentration of 0.05% (v/v). For analyses of the frequencies of shoot regeneration, three biological replicates were performed. For each replicate, root explants from more than 100 individuals were used. Different plants were used between distinct replicates. For transgenic plants, separate lines were used in each replicate. Regenerated shoots were defined as described previously (Daimon et al., 2003). The tissues containing a meristem surrounded by three or more leaves or leaf primordia with a phyllotactic pattern were defined as a shoot.

For analyses of stage-specific silencing of *ARR*s, explants were transferred to SIM media containing 0.05% (v/v) ethanol at 0, 4, 8, or 12 d of SIM incubation, and the shoot regeneration percentages were determined.

The 24-h ethanol induction was performed on *gWUS-GFP*$_3$ transgenic explants at days 0, 4, 8, and 12 of SIM incubation. The *gWUS-GFP*$_3$ signals were then visualized using confocal microscopy as described below.

For the complementary experiment, *Pro35S:WUS* was transformed into the *arr1 12* double mutant to generate the *Pro35S:WUS arr1 12* lines. The shoot regeneration frequency was then determined as above.

Confocal Microscopy

Callus at different days of incubation in SIM that was ~5 to 8 mm in diameter was selected using an Olympus SZX-16 stereomicroscope (Olympus) and cut into sections 1 to 2 mm thick along the longitudinal axis. The sections were then observed, and fluorescent images were captured using a Leica TCS SP5II confocal laser scanning microscope with a 40× oil objective. Multitracking in line scan mode and a 488/561 main dichroic filter were used to image GFP and dsRED together (Heisler et al., 2005). A 561-nm laser line and a 600- to 640-nm band-pass filter were used for dsRED, and a 488-nm laser line and a 505- to 550-nm band-pass filter were used for GFP.

Histochemical GUS Assay

Histochemical GUS assays were performed on transgenic Arabidopsis lines expressing *ProARR1:GUS* in the wild type, lines expressing *ProYUC1:GUS* in the wild type, *arr1 10* and *arr1 12* double mutants, and lines expressing *ProYUC4:GUS* in the wild type and *arr10 12* double mutants. For GUS staining, callus at different days on SIM were harvested and fixed in 90% acetone on ice for 15 min. Each callus was then transferred into GUS staining buffer containing 50 mM $NaPO_4$ (pH 7.2), 2 mM X-gluc (Sigma-Aldrich), 0.5 mM $K_3Fe(CN)_6$, and 0.5 mM $K_4Fe(CN)_6$, vacuum infiltrated, and incubated at 37°C overnight. The stained callus was photographed using an Olympus SZX-16 stereomicroscope equipped with an Olympus DP72 digital camera. For anatomical analysis, stained callus was dehydrated for 1 h for each in 70, 80, 90, and 100% ethanol and embedded in paraffin (Sigma-Aldrich). Embedded callus samples were then sectioned at 8 μm, and paraffin was removed by incubation in xylene. Finally, the sections were stained with 0.2% ruthenium red and photographed using an Olympus BX-51 microscope equipped with an Olympus DP71 digital camera.

RT-qPCR

Total RNA was extracted using the TRI reagent (Sigma-Aldrich). The full-length cDNA was generated with the RevertAid first-strand cDNA synthesis kit (Thermo). RT-qPCR was performed on a Chromo4 real-time PCR system (Bio-Rad) using SuperReal PreMix Plus (Tiangen) with gene-specific primers. The transcript levels of the genes in each sample were normalized to that of the housekeeping gene *TUBULIN2*, and the values shown are the mean ± SD of three biological replicates. For Figures 2A, 2C, and 6A, callus tissues at different days of SIM incubation were used. Tissues derived from different plants were used in distinct replicates. For Supplemental Figures 2 and 9C, inflorescences of 35-d-old seedlings were used. Tissues used between distinct replicates were generated from different plants. The primers are listed in Supplemental Data Set 1.

In Situ Hybridization

Callus at different days on SIM was collected and fixed in FAA (10% formaldehyde, 5% acetic acid, and 50% alcohol) at 4°C overnight. The fixed tissues were embedded in Paraplast (Sigma-Aldrich) after dehydration and were then sectioned at 8 μm. RNA probes were synthesized and labeled in vitro, and the hybridized signals were detected as previously described (Zhao et al., 2006). Photographs were taken using an Olympus BX-51 microscope equipped with an Olympus DP71 digital camera.

ChIP Assay

ChIP assays were performed using an EZ-ChIP Kit (Upstate) according to the manufacturer's protocol. Callus tissues incubated for various days on SIM (Figures 5 and 8; Supplemental Figure 7) or shoots (without leaves and cotyledons) from seedlings at 10 d after germination (Figure 9; Supplemental Figure 11) of the *ProARR1:ARR1-GFP*, *ProARR10:ARR10-GFP*, and *ProARR12:ARR12-GFP* transgenic lines were used for ChIP

analyses. For each replicate, 0.3 g of tissue was harvested and cross-linked with 1% (v/v) formaldehyde in GB buffer (0.4 M sucrose, 10 mM Tris, pH 8.0, 1 mM EDTA, pH 8.0, and 1 mM PMSF) under a vacuum for 10 min at room temperature. The cross-linking was quenched with 125 mM glycine. The chromatin was then resuspended and sheared by sonication to produce DNA fragments of between 0.2 and 1 kb. The chromatin complexes were immunoprecipitated with anti-GFP antibody (Sigma-Aldrich; lot no. PM1008202, catalog no. SAB5300167). Finally, the precipitated DNA fragments were analyzed using RT-qPCR as described previously (Cheng et al., 2014; Zhou et al., 2009). Tissues derived from different plants were used in distinct biological replicates. The ARR binding elements have been described previously (Sakai et al., 2000; Bhargava A et al., 2013; Kieber and Schaller, 2014). The primers used for qPCR analyses are listed in Supplemental Data Set 1, and the sequences of fragments are listed in Supplemental Data Set 2.

EMSA

The DNA fragments encoding DNA binding domains of ARR1, ARR10, and ARR12 (amino acids 236–299 for ARR1, amino acids 183–235 for ARR10, and amino acids 195–248 for ARR12) were inserted into pGEX-4T-1 vector digested with *Bam*HI and *Xho*I, which was then expressed in the *Escherichia coli* BL21 (DE3) cell line to produce GST-tagged ARR protein. The recombinant fusion protein was purified using Glutathione Sepharose 4B (GE Healthcare) following the manufacturer's instructions. Annealed double-stranded oligonucleotides containing putative binding sequences were labeled with biotin. The LightShift Chemiluminescent EMSA Kit (Thermo) was used for binding reactions. The labeled complex was detected using a Chemiluminescent Nucleic Acid Detection Module (Thermo). The competition experiments were performed with different amounts of nonlabeled oligonucleotides. The mutated competitors in Figures 5B and 8B were generated by replacing two base pairs in the ARR binding elements (GATC/T to CTTC/T). Primers and oligonucleotide probe sequences are listed in Supplemental Data Sets 1 and 2.

Yeast One-Hybrid Assays

Yeast one-hybrid assays were performed as previously described (Cheng et al., 2013). *WUS*-3 (−394 to −566 bp upstream of the ATG start codon) and *YUC4*-2 (−742 to −913 bp upstream of the ATG start codon) fragments were cloned into the pAbAi vector digested with *Hind*III and *Kpn*I, creating *WUS*-3-AbAi and *YUC4*-2-AbAi. *WUS*-3-AbAi, *YUC4*-2-AbAi, and p53-AbAi (positive control; Clontech Laboratories) were linearized by digestion with *Bbs*I prior to transformation of the yeast strain Y1H Gold. The full-length cDNA of *ARR1*, *ARR10*, and *ARR12* was isolated and cloned into the pDEST-GADT7 activation domain (AD) vector, creating the pAD-ARR1, pAD-ARR10, and pAD-ARR12 plasmid. The p53 sequence was cloned into the pDEST-GADT7 activation domain (AD) vector, creating the pAD-p53 positive control. The pAD-ARR1, pAD-ARR10, and pAD-ARR12 or empty pDEST-GADT7 vector as negative control was subsequently transformed into the yeast strain containing the *WUS*-3-AbAi or *YUC4*-2-AbAi constructs. Activation of the yeast was observed after 3 d on selection plates (synthetic dextrose/-Leu) containing 600 ng mL^{-1} aureobasidin A. The primers are described in Supplemental Data Set 1. Oligonucleotide sequences are listed in Supplemental Data Set 2.

Transient Expression Assay

The coding sequences of *ARR1*, *ARR10*, and *ARR12* were cloned into the pGreenII 62-SK vector downstream of the *Pro35S* promoter and were used as effectors. A 2479-bp fragment upstream of the start codon of *WUS* or mutated *WUS* promoters were introduced into the pGreenII 0800-LUC vector upstream of *LUC*, and these constructs were used as the reporters. The pGreenII 0800-LUC vector harboring the renilla luciferase (REN) gene under the control of the *Pro35S* promoter was used as the internal control. Protoplast transient expression assays were performed as previously described (Song et al., 2014). Mesophyll protoplast preparation and transfection were performed according to a previously reported method (Yoo et al., 2007). For transient expression assays in tobacco leaves, leaves of *Nicotiana benthamiana* were transiently transformed and examined as previously described (Guo et al., 2015). Biological replicates represent the results of three independent assays. For transient expression in tobacco leaves, three leaves from different plants were used in one replicate. Protoplasts used in the three replicates were obtained from different plants.

Histological Analyses of the SAM

The SAMs from wild-type and *arr1 10 12* mutant seedlings at 14 d after germination were used for *gWUS-GFP*$_3$ expression analyses. The intensity of fluorescence was measured using ImageJ software (Córdoba et al., 2016). The shoot meristem width was measured at the maximum width between leaf primordia. ImageJ software was used for measuring shoot meristem width and counting cell number (Maes et al., 2008; Vidal et al., 2010).

Accession Numbers

Sequence data from this article can be found in the Arabidopsis Genome Initiative under the following accession numbers: *ARR1* (At3g16857), *ARR2* (At4g16110), *ARR10* (At4g31920), *ARR11* (At1g67710), *ARR12* (At2g25180), *ARR13* (AT2G27070), *ARR18* (At5g58080), *ARR21* (AT5G07210), *WUS* (At2g17950), *YUC1* (AT4G32540), *YUC2* (AT4G13260), *YUC4* (AT5G11320), and *YUC6* (AT5G25620).

Supplemental Data

Supplemental Figure 1. Expression Patterns of *ARR1* during Shoot Regeneration.

Supplemental Figure 2. The Effectiveness of Artificial MicroRNAs against *ARR1*, *ARR10*, and *ARR12*.

Supplemental Figure 3. Defects in *ARR1*, *ARR10*, and *ARR12* Attenuate Shoot Regeneration.

Supplemental Figure 4. Transient Expressing *ARR1*, *ARR10*, or *ARR12* Activates *WUS* Transcription.

Supplemental Figure 5. Mutating the ARR Binding Elements in *WUS* Promoter Region Reduced ARR-Mediated *WUS* Transcription.

Supplemental Figure 6. Mutations in *ARRs* Enhanced the Signals of the *pYUC1:GUS* and *pYUC4:GUS* Reporters.

Supplemental Figure 7. ARR1 Binds the Promoter of *YUC1* and Regulates Its Transcription.

Supplemental Figure 8. Expression Patterns of *ProDR5:GFP* Were Disturbed in *YUC4ox* Lines.

Supplemental Figure 9. *YUCs* Act Downstream of *ARRs*.

Supplemental Figure 10. Expression of *YUC4* under Mutated *YUC4* Promoter Reduced Shoot Regeneration.

Supplemental Figure 11. ARR1, ARR10, and ARR12 Bind the Promoters of *YUCs* and Regulate Their Expression in the SAM.

Supplemental Figure 12. Phenotypes of *pARR10:YUC4* Transgenic Lines.

Supplemental Figure 13. *ARR1*, *ARR10*, and *ARR12* Are Involved in Axillary Meristem Initiation.

Supplemental Data Set 1. Primers Used in This Study.

Supplemental Data Set 2. Oligo Sequences Used in the Yeast One-Hybrid, EMSA, and ChIP Assays.

ACKNOWLEDGMENTS

We thank the ABRC for providing the plant materials. We thank E.M. Meyerowitz (California Institute of Technology), T. Laux (University of Freiburg), and Y. Zhao (University of California at San Diego) for providing materials. This work was supported by the National Natural Sciences Foundation of China (91217308, 90917015, and 31570281).

AUTHOR CONTRIBUTIONS

X.S.Z., Z.J.C., and Y.L.S. conceived and designed the experiments. W.J.M. and Z.J.C. performed the experiments and data analysis with the help of M.M.Z., X.F.R., Z.W.W., and Y.Y.T. in the laboratory of X.S.Z. X.S.Z. and Y.L.S. wrote the manuscript. X.S.Z. supervised the project.

Received August 15, 2016; revised April 25, 2017; accepted May 31, 2017; published June 2, 2017.

REFERENCES

Aichinger, E., Kornet, N., Friedrich, T., and Laux, T. (2012). Plant stem cell niches. Annu. Rev. Plant Biol. **63:** 615–636.

Bäurle, I., and Laux, T. (2005). Regulation of *WUSCHEL* transcription in the stem cell niche of the Arabidopsis shoot meristem. Plant Cell **17:** 2271–2280.

Besnard, F., et al. (2014). Cytokinin signalling inhibitory fields provide robustness to phyllotaxis. Nature **505:** 417–421.

Bhargava, A., Clabaugh, I., To, J.P., Maxwell, B.B., Chiang, Y.H., Schaller, G.E., Loraine, A., and Kieber, J.J. (2013). Identification of cytokinin-responsive genes using microarray meta-analysis and RNA-Seq in Arabidopsis. Plant Physiol. **162:** 272–294.

Bishopp, A., Help, H., El-Showk, S., Weijers, D., Scheres, B., Friml, J., Benková, E., Mähönen, A.P., and Helariutta, Y. (2011). A mutually inhibitory interaction between auxin and cytokinin specifies vascular pattern in roots. Curr. Biol. **21:** 917–926.

Brand, U., Fletcher, J.C., Hobe, M., Meyerowitz, E.M., and Simon, R. (2000). Dependence of stem cell fate in *Arabidopsis* on a feedback loop regulated by *CLV3* activity. Science **289:** 617–619.

Buechel, S., Leibfried, A., To, J.P., Zhao, Z., Andersen, S.U., Kieber, J.J., and Lohmann, J.U. (2010). Role of A-type *ARABIDOPSIS RESPONSE REGULATORS* in meristem maintenance and regeneration. Eur. J. Cell Biol. **89:** 279–284.

Chandler, J.W., and Werr, W. (2015). Cytokinin-auxin crosstalk in cell type specification. Trends Plant Sci. **20:** 291–300.

Chatfield, S.P., Capron, R., Severino, A., Penttila, P.A., Alfred, S., Nahal, H., and Provart, N.J. (2013). Incipient stem cell niche conversion in tissue culture: using a systems approach to probe early events in *WUSCHEL*-dependent conversion of lateral root primordia into shoot meristems. Plant J. **73:** 798–813.

Cheng, Y., Dai, X., and Zhao, Y. (2006). Auxin biosynthesis by the YUCCA flavin monooxygenases controls the formation of floral organs and vascular tissues in *Arabidopsis.* Genes Dev. **20:** 1790–1799.

Cheng, Z.J., Zhao, X.Y., Shao, X.X., Wang, F., Zhou, C., Liu, Y.G., Zhang, Y., and Zhang, X.S. (2014). Abscisic acid regulates early seed development in *Arabidopsis* by ABI5-mediated transcription of *SHORT HYPOCOTYL UNDER BLUE1.* Plant Cell **26:** 1053–1068.

Cheng, Z.J., et al. (2013). Pattern of auxin and cytokinin responses for shoot meristem induction results from the regulation of cytokinin biosynthesis by AUXIN RESPONSE FACTOR3. Plant Physiol. **161:** 240–251.

Córdoba, J.P., Marchetti, F., Soto, D., Martin, M.V., Pagnussat, G.C., and Zabaleta, E. (2016). The CA domain of the respiratory complex I is required for normal embryogenesis in *Arabidopsis thaliana*. J. Exp. Bot. **67:** 1589–1603.

Daimon, Y., Takabe, K., and Tasaka, M. (2003). The *CUP-SHAPED COTYLEDON* genes promote adventitious shoot formation on calli. Plant Cell Physiol. **44:** 113–121.

Daum, G., Medzihradszky, A., Suzaki, T., and Lohmann, J.U. (2014). A mechanistic framework for noncell autonomous stem cell induction in *Arabidopsis.* Proc. Natl. Acad. Sci. USA **111:** 14619–14624.

De Rybel, B., Mähönen, A.P., Helariutta, Y., and Weijers, D. (2016). Plant vascular development: from early specification to differentiation. Nat. Rev. Mol. Cell Biol. **17:** 30–40.

Domagalska, M.A., and Leyser, O. (2011). Signal integration in the control of shoot branching. Nat. Rev. Mol. Cell Biol. **12:** 211–221.

Duclercq, J., Sangwan-Norreel, B., Catterou, M., and Sangwan, R.S. (2011). De novo shoot organogenesis: from art to science. Trends Plant Sci. **16:** 597–606.

Efroni, I., Mello, A., Nawy, T., Ip, P.L., Rahni, R., DelRose, N., Powers, A., Satija, R., and Birnbaum, K.D. (2016). Root regeneration triggers an embryo-like sequence guided by hormonal interactions. Cell **165:** 1721–1733.

Fletcher, J.C., and Meyerowitz, E.M. (2000). Cell signaling within the shoot meristem. Curr. Opin. Plant Biol. **3:** 23–30.

Gaillochet, C., Daum, G., and Lohmann, J.U. (2015). O cell, where art thou? The mechanisms of shoot meristem patterning. Curr. Opin. Plant Biol. **23:** 91–97.

Gordon, S.P., Chickarmane, V.S., Ohno, C., and Meyerowitz, E.M. (2009). Multiple feedback loops through cytokinin signaling control stem cell number within the Arabidopsis shoot meristem. Proc. Natl. Acad. Sci. USA **106:** 16529–16534.

Gordon, S.P., Heisler, M.G., Reddy, G.V., Ohno, C., Das, P., and Meyerowitz, E.M. (2007). Pattern formation during de novo assembly of the *Arabidopsis* shoot meristem. Development **134:** 3539–3548.

Guo, D., Zhang, J., Wang, X., Han, X., Wei, B., Wang, J., Li, B., Yu, H., Huang, Q., Gu, H., Qu, L.J., and Qin, G. (2015). The WRKY transcription factor WRKY71/EXB1 controls shoot branching by transcriptionally regulating *RAX* genes in Arabidopsis. Plant Cell **27:** 3112–3127.

Heisler, M.G., Ohno, C., Das, P., Sieber, P., Reddy, G.V., Long, J.A., and Meyerowitz, E.M. (2005). Patterns of auxin transport and gene expression during primordium development revealed by live imaging of the *Arabidopsis* inflorescence meristem. Curr. Biol. **15:** 1899–1911.

Hill, K., Mathews, D.E., Kim, H.J., Street, I.H., Wildes, S.L., Chiang, Y.H., Mason, M.G., Alonso, J.M., Ecker, J.R., Kieber, J.J., and Schaller, G.E. (2013). Functional characterization of type-B response regulators in the Arabidopsis cytokinin response. Plant Physiol. **162:** 212–224.

Hwang, I., Sheen, J., and Müller, B. (2012). Cytokinin signaling networks. Annu. Rev. Plant Biol. **63:** 353–380.

Ikeda, M., Mitsuda, N., and Ohme-Takagi, M. (2009). *Arabidopsis* WUSCHEL is a bifunctional transcription factor that acts as a repressor in stem cell regulation and as an activator in floral patterning. Plant Cell **21:** 3493–3505.

Ikeuchi, M., Ogawa, Y., Iwase, A., and Sugimoto, K. (2016). Plant regeneration: cellular origins and molecular mechanisms. Development **143:** 1442–1451.

Ishida, K., Yamashino, T., Yokoyama, A., and Mizuno, T. (2008). Three type-B response regulators, ARR1, ARR10 and ARR12, play essential but redundant roles in cytokinin signal transduction throughout the life cycle of *Arabidopsis thaliana.* Plant Cell Physiol. **49:** 47–57.

Iwase, A., Mitsuda, N., Koyama, T., Hiratsu, K., Kojima, M., Arai, T., Inoue, Y., Seki, M., Sakakibara, H., Sugimoto, K., and Ohme-Takagi, M. (2011). The AP2/ERF transcription factor WIND1 controls cell dedifferentiation in Arabidopsis. Curr. Biol. **21:** 508–514.

Iwase, A., Harashima, H., Ikeuchi, M., Rymen, B., Ohnuma, M., Komaki, S., Morohashi, K., Kurata, T., Nakata, M., Ohme-Takagi, M., Grotewold, E., and Sugimoto, K. (2017). WIND1 promotes shoot regeneration through transcriptional activation of *ENHANCER OF SHOOT REGENERATION1* in Arabidopsis. Plant Cell **29:** 54–69.

Kareem, A., Durgaprasad, K., Sugimoto, K., Du, Y., Pulianmackal, A.J., Trivedi, Z.B., Abhayadev, P.V., Pinon, V., Meyerowitz, E.M., Scheres, B., and Prasad, K. (2015). *PLETHORA* genes control regeneration by a two-step mechanism. Curr. Biol. **25:** 1017–1030.

Kerstetter, R.A., and Hake, S. (1997). Shoot meristem formation in vegetative development. Plant Cell **9:** 1001–1010.

Kieber, J.J., and Schaller, G.E. (2014). Cytokinins. Arabidopsis Book **12:** e0168.

Laux, T. (2003). The stem cell concept in plants: a matter of debate. Cell **113:** 281–283.

Laux, T., Würschum, T., and Breuninger, H. (2004). Genetic regulation of embryonic pattern formation. Plant Cell **16 (suppl.):** S190–S202.

Leibfried, A., To, J.P., Busch, W., Stehling, S., Kehle, A., Demar, M., Kieber, J.J., and Lohmann, J.U. (2005). WUSCHEL controls meristem function by direct regulation of cytokinin-inducible response regulators. Nature **438:** 1172–1175.

Liu, X., Dinh, T.T., Li, D., Shi, B., Li, Y., Cao, X., Guo, L., Pan, Y., Jiao, Y., and Chen, X. (2014). *AUXIN RESPONSE FACTOR 3* integrates the functions of *AGAMOUS* and *APETALA2* in floral meristem determinacy. Plant J. **80:** 629–641.

Maes, L., Inzé, D., and Goossens, A. (2008). Functional specialization of the TRANSPARENT TESTA GLABRA1 network allows differential hormonal control of laminal and marginal trichome initiation in Arabidopsis rosette leaves. Plant Physiol. **148:** 1453–1464.

Mason, M.G., Li, J., Mathews, D.E., Kieber, J.J., and Schaller, G.E. (2004). Type-B response regulators display overlapping expression patterns in Arabidopsis. Plant Physiol. **135:** 927–937.

Mayer, K.F., Schoof, H., Haecker, A., Lenhard, M., Jürgens, G., and Laux, T. (1998). Role of *WUSCHEL* in regulating stem cell fate in the *Arabidopsis* shoot meristem. Cell **95:** 805–815.

Moreno-Risueno, M.A., Sozzani, R., Yardımcı, G.G., Petricka, J.J., Vernoux, T., Blilou, I., Alonso, J., Winter, C.M., Ohler, U., Scheres, B., and Benfey, P.N. (2015). Transcriptional control of tissue formation throughout root development. Science **350:** 426–430.

Müller, B., and Sheen, J. (2008). Cytokinin and auxin interaction in root stem-cell specification during early embryogenesis. Nature **453:** 1094–1097.

Nieminen, K., Blomster, T., Helariutta, Y., and Mähönen, A.P. (2015). Vascular cambium development. Arabidopsis Book **13:** e0177.

Riou-Khamlichi, C., Huntley, R., Jacqmard, A., and Murray, J.A. (1999). Cytokinin activation of *Arabidopsis* cell division through a D-type cyclin. Science **283:** 1541–1544.

Sakai, H., Aoyama, T., and Oka, A. (2000). *Arabidopsis* ARR1 and ARR2 response regulators operate as transcriptional activators. Plant J. **24:** 703–711.

Sakai, H., Honma, T., Aoyama, T., Sato, S., Kato, T., Tabata, S., and Oka, A. (2001). ARR1, a transcription factor for genes immediately responsive to cytokinins. Science **294:** 1519–1521.

Schaller, G.E., Bishopp, A., and Kieber, J.J. (2015). The yin-yang of hormones: cytokinin and auxin interactions in plant development. Plant Cell **27:** 44–63.

Schoof, H., Lenhard, M., Haecker, A., Mayer, K.F., Jürgens, G., and Laux, T. (2000). The stem cell population of *Arabidopsis* shoot meristems in maintained by a regulatory loop between the *CLAVATA* and *WUSCHEL* genes. Cell **100:** 635–644.

Sena, G., Wang, X., Liu, H.Y., Hofhuis, H., and Birnbaum, K.D. (2009). Organ regeneration does not require a functional stem cell niche in plants. Nature **457:** 1150–1153.

Skoog, F., and Miller, C.O. (1957). Chemical regulation of growth and organ formation in plant tissues cultured in vitro. Symp. Soc. Exp. Biol. **11:** 118–130.

Song, S., Huang, H., Gao, H., Wang, J., Wu, D., Liu, X., Yang, S., Zhai, Q., Li, C., Qi, T., and Xie, D. (2014). Interaction between MYC2 and ETHYLENE INSENSITIVE3 modulates antagonism between jasmonate and ethylene signaling in *Arabidopsis.* Plant Cell **26:** 263–279.

Sugimoto, K., Jiao, Y., and Meyerowitz, E.M. (2010). Arabidopsis regeneration from multiple tissues occurs via a root development pathway. Dev. Cell **18:** 463–471.

Tucker, M.R., Hinze, A., Tucker, E.J., Takada, S., Jürgens, G., and Laux, T. (2008). Vascular signalling mediated by ZWILLE potentiates WUSCHEL function during shoot meristem stem cell development in the *Arabidopsis* embryo. Development **135:** 2839–2843.

Vidal, E.A., Araus, V., Lu, C., Parry, G., Green, P.J., Coruzzi, G.M., and Gutiérrez, R.A. (2010). Nitrate-responsive miR393/*AFB3* regulatory module controls root system architecture in *Arabidopsis thaliana.* Proc. Natl. Acad. Sci. USA **107:** 4477–4482.

Wang, Y., Wang, J., Shi, B., Yu, T., Qi, J., Meyerowitz, E.M., and Jiao, Y. (2014). The stem cell niche in leaf axils is established by auxin and cytokinin in *Arabidopsis.* Plant Cell **26:** 2055–2067.

Yadav, R.K., Tavakkoli, M., and Reddy, G.V. (2010). WUSCHEL mediates stem cell homeostasis by regulating stem cell number and patterns of cell division and differentiation of stem cell progenitors. Development **137:** 3581–3589.

Yadav, R.K., Perales, M., Gruel, J., Girke, T., Jönsson, H., and Reddy, G.V. (2011). WUSCHEL protein movement mediates stem cell homeostasis in the *Arabidopsis* shoot apex. Genes Dev. **25:** 2025–2030.

Yoo, S.D., Cho, Y.H., and Sheen, J. (2007). *Arabidopsis* mesophyll protoplasts: a versatile cell system for transient gene expression analysis. Nat. Protoc. **2:** 1565–1572.

Zhang, T.Q., Lian, H., Tang, H., Dolezal, K., Zhou, C.M., Yu, S., Chen, J.H., Chen, Q., Liu, H., Ljung, K., and Wang, J.W. (2015). An intrinsic microRNA timer regulates progressive decline in shoot regenerative capacity in plants. Plant Cell **27:** 349–360.

Zhang, W., Swarup, R., Bennett, M., Schaller, G.E., and Kieber, J.J. (2013). Cytokinin induces cell division in the quiescent center of the *Arabidopsis* root apical meristem. Curr. Biol. **23:** 1979–1989.

Zhao, X.Y., Cheng, Z.J., and Zhang, X.S. (2006). Overexpression of *TaMADS1*, a *SEPALLATA*-like gene in wheat, causes early flowering and the abnormal development of floral organs in Arabidopsis. Planta **223:** 698–707.

Zhao, Y., Christensen, S.K., Fankhauser, C., Cashman, J.R., Cohen, J.D., Weigel, D., and Chory, J. (2001). A role for flavin monooxygenase-like enzymes in auxin biosynthesis. Science **291:** 306–309.

Zhao, Z., Andersen, S.U., Ljung, K., Dolezal, K., Miotk, A., Schultheiss, S.J., and Lohmann, J.U. (2010). Hormonal control of the shoot stem-cell niche. Nature **465:** 1089–1092.

Zhou, Y., Zhang, X., Kang, X., Zhao, X., Zhang, X., and Ni, M. (2009). SHORT HYPOCOTYL UNDER BLUE1 associates with *MINISEED3* and *HAIKU2* promoters in vivo to regulate *Arabidopsis* seed development. Plant Cell **21:** 106–117.

Zhou, Y., Liu, X., Engstrom, E.M., Nimchuk, Z.L., Pruneda-Paz, J.L., Tarr, P.T., Yan, A., Kay, S.A., and Meyerowitz, E.M. (2015). Control of plant stem cell function by conserved interacting transcriptional regulators. Nature **517:** 377–380.

Zürcher, E., Tavor-Deslex, D., Lituiev, D., Enkerli, K., Tarr, P.T., and Müller, B. (2013). A robust and sensitive synthetic sensor to monitor the transcriptional output of the cytokinin signaling network in planta. Plant Physiol. **161:** 1066–1075.